

Stroboscopic Invariants in Storage Rings with Synchrotron Motion

S. Webb,^{a,1} N. Cook,^a J. Eldred^b

^a*RadiaSoft LLC,
3380 Mitchell Lane, Boulder, CO, USA*

^b*Fermi National Accelerator Laboratory,
Batavia, IL, USA*

E-mail: swebb@radiasoft.net

ABSTRACT: In an ideal accelerator, the single-particle dynamics can be decoupled into transverse motion – the betatron oscillations – and longitudinal motion – the synchrotron oscillations. Chromatic and dispersive effects introduce a coupling between these dynamics, the so-called synchro-betatron coupling. We present an analysis of the fully coupled dynamics over a single synchrotron oscillation that leads to a stroboscopic invariant with synchro-betatron coupling in a generic lattice. This invariant is correct to $\mathcal{O}(\nu_s)$, where ν_s is the synchrotron tune. We apply this analysis to a design for a rapid cycling synchrotron built using the integrable optics described by Danilov and Nagaitsev, showing that although there is fairly complex behavior over the course of a synchrotron oscillation, the predicted invariants are nevertheless periodic with the synchrotron motion.

KEYWORDS: Beam Dynamics, Beam Optics

¹Corresponding author.

Contents

1	Introduction	1
2	Synchro-betatron Coupling	2
3	A Stroboscopic Hamiltonian	2
4	Stroboscopic Invariants in an Integrable Rapid-Cycling Synchrotron	6
5	Discussion	8
A	Symplectic Maps, Lie Algebras, and the Baker-Campbell-Hausdorff Formula	9
B	Leading Order Correction	10

1 Introduction

Single-particle dynamics in particle accelerators can be broken into the fast transverse betatron oscillations, with tunes $\nu_{x,y} \gg 1$, and the much slower synchrotron oscillations, with tunes $\nu_s \ll 1$. For a coasting beam, the momentum dependence of the focusing element strengths leads to chromaticity, a momentum-dependent betatron tune, and dispersion, a momentum-dependent closed orbit. When an rf cavity is added and synchrotron motion occurs, that synchrotron motion couples to the betatron motion through the chromaticity and dispersion – so-called synchro-betatron coupling.

Synchro-betatron coupling can lead to complex coupled dynamics. The impact of synchro-betatron coupling has been well-studied for linear alternating gradient focusing lattices [1–3], but their influence on more novel lattice designs, such as nonlinear integrable optics [4–7], has yet to be studied in detail.

In this paper, we calculate a stroboscopic invariant of coupled synchro-betatron motion in the limit of small synchrotron tune. This invariant is the Hamiltonian that generates an N -turn map, where $N\nu_s \approx 1$. We show that this Hamiltonian is correct to $\mathcal{O}(\nu_s)$, and that the perturbing terms do not cause secular growth in the invariants. This Hamiltonian is a pure function of the transverse coordinates and the synchrotron action coordinate – thus if this Hamiltonian is integrable then the entire system is integrable over N turns. We demonstrate the preservation of integrable dynamics in the context of an integrable rapid cycling synchrotron, designed to use nonlinear integrable optics to mitigate beam loss due to coherent instabilities in high intensity proton beams. This result relies on the single-turn Lie map formalism of Dragt *et al.* [8–14], and therefore we give a brief survey of key results in Appendix A.

2 Synchro-betatron Coupling

The simplest model for single-particle dynamics in a particle accelerator is the uncoupled vertical and horizontal betatron oscillations, with independent synchrotron motion longitudinally. Dispersion can complicate this picture, as each trajectory's momentum-dependent closed orbit oscillates with the synchrotron motion. The simplest linear cases creates normal modes that couple transverse and longitudinal motion, and the eigenemittances and tunes can be computed with a generic symplectic matrix formulation [15]. The next-leading-order dynamics comes from chromaticity, the momentum dependence of the betatron tune. Because the system is Hamiltonian, a betatron tune that depends on the momentum implies a betatron amplitude dependence in the synchrotron tune – so-called *synchro-betatron coupling*.

This coupling has a number of implications. The slow change in the momentum offset of a particle's trajectory suggests that there will also be a slow change in the chromaticity – the synchrotron motion will modulate the betatron oscillations with a frequency of the betatron phase. Synchro-betatron coupling therefore can lead to sidebands in the betatron motion located at $\nu_{\perp} \pm m\nu_s$ for betatron tune ν_{\perp} and synchrotron tune ν_s [1, 2]. Because of the coupling in the system, the synchrotron motion modifies the usual transverse action-angle variables [3]. This can lead to synchro-betatron coupling induced parametric resonances when the betatron tune is a harmonic of the synchrotron tune.

Synchro-betatron coupling is conceptually similar to adiabatic analysis in that a quantity that affects the transverse motion is changing slowly compared to the transverse oscillations. Because the synchrotron oscillations are slow and periodic, we expect to be able to find a period-averaged Hamiltonian treatment of synchro-betatron coupling. However, because the slowly changing quantity is a dynamical quantity in a Hamiltonian system, the analysis is more subtle – we must make sure any treatment of synchro-betatron coupling reflects the Hamiltonian nature of the dynamics.

3 A Stroboscopic Hamiltonian

Synchrotron motion in the absence of coupling is a periodic system, slowly varying compared to the much faster betatron oscillations. The periodicity of the synchrotron motion suggests looking at the total dynamics stroboscopically, looking every N turns where $N \times \nu_s \approx 1$ to analyze a sort of synchrotron-period-averaged influence on the transverse dynamics.

Suppose we have a storage ring comprised of a sequence of transverse elements and a single, thin rf cavity. The single-turn map takes the form

$$\mathcal{M} = \mathcal{M}_{\perp} \mathcal{M}_V \tag{3.1}$$

where the Hamiltonian that generates \mathcal{M}_{\perp} is of the form

$$H = H_{\perp}(\vec{z}_{\perp}, \delta) + \alpha_c(\delta) \tag{3.2}$$

and the rf potential that generates the thin cavity map \mathcal{M}_V is generated by $V(\phi)$. Here δ and ϕ are canonically conjugate, α_c captures the momentum compaction of the ring, and H_{\perp} describes the transverse motion with chromatic and dispersive effects. Because α_c commutes with H_{\perp} , we can

factor this into three maps: $\mathcal{M}_\perp \mathcal{M}_c \mathcal{M}_V$, where H_\perp generates \mathcal{M}_\perp , α_c generates \mathcal{M}_c , and \mathcal{M}_V is as before. In the absence of synchro-betatron coupling, the transverse dynamics are specified entirely by \mathcal{M}_\perp and the longitudinal dynamics are specified entirely by the synchrotron map $\mathcal{M}_s = \mathcal{M}_c \mathcal{M}_V$.

We assume the synchrotron motion is integrable, so the dynamics can be specified in action-angle coordinates (A, ψ) , and

$$\mathcal{M}_s = \exp\{-:h_s(A):\} \quad (3.3)$$

with amplitude-dependent synchrotron phase advance $\mu_s(A)$. Because the synchrotron motion is presumed integrable, we know that δ must be a periodic function with the synchrotron phase, and can be written as a Fourier series

$$\delta = \sum_m \delta_m(A) e^{im\psi}. \quad (3.4)$$

The full single-turn map is therefore

$$\mathcal{M} = \exp\{-:H_\perp(\vec{z}_\perp; A, \psi):\} \exp\{-:h_s(A_s):\}. \quad (3.5)$$

Once again, because δ is periodic with the synchrotron phase, so too is H_\perp , and we can rewrite

$$H_\perp = \sum_{k=-\infty}^{\infty} h_k(\vec{z}_\perp, A) e^{ik\psi} = \overline{H}(\vec{z}_\perp, A) + \sum_{k \neq 0} h_k(\vec{z}_\perp, A) e^{ik\psi} \quad (3.6)$$

where we have called out $\overline{H} = \langle H_\perp \rangle_{\psi_s}$, the average of H_\perp over the synchrotron phase, as it will be important later. That H_\perp is a real function requires that \overline{H} be real, and that $h_{-k} = h_k^*$.

For stroboscopic dynamics, we want to look at an N -turn map, given by

$$\mathcal{M}^N = (\mathcal{M}_\perp \mathcal{M}_s)^N. \quad (3.7)$$

Through a judicious insertion of an identity operator, we can move all of the synchrotron motion maps to the left, and leave only the transverse dynamics to the right. This can be accomplished by noting that

$$\begin{aligned} \mathcal{M}_\perp \mathcal{M}_s \mathcal{M}_\perp \mathcal{M}_s &= \mathcal{M}_\perp \mathcal{M}_s \mathcal{M}_s \mathcal{M}_s^{-1} \mathcal{M}_\perp \mathcal{M}_s \\ &= \mathcal{M}_\perp \mathcal{M}_s^2 \tilde{\mathcal{M}}_\perp^{(1)} \end{aligned} \quad (3.8)$$

where $\tilde{\mathcal{M}}_\perp^{(n)} = \mathcal{M}_s^{-n} \mathcal{M}_\perp \mathcal{M}_s^n$. It is straightforward to show that, by moving each successive synchrotron map to the left in this process, we get the N -turn map

$$\mathcal{M}^N = (\mathcal{M}_s)^N \left(\prod_{n=N}^1 \tilde{\mathcal{M}}_\perp^{(n)} \right) \quad (3.9)$$

where we are counting the index down from left to right.

From the similarity transformation identity described in Appendix A, it is straightforward to compute $\tilde{\mathcal{M}}_\perp^{(n)}$. The similarity transformation moves the synchrotron motion into the argument of

the \mathcal{M}_\perp exponential, thus:

$$\begin{aligned}
\tilde{\mathcal{M}}_\perp^{(n)} &= \mathcal{M}_s^{-n} \mathcal{M}_\perp \mathcal{M}_s^n \\
&= \mathcal{M}_s^{-n} \exp \left\{ - : \sum_{k=-\infty}^{\infty} h_k(\vec{z}_\perp, A) e^{ik\psi} : \right\} \mathcal{M}_s^{-n} \\
&= \exp \left\{ - : \mathcal{M}_s^{-n} \sum_{k=-\infty}^{\infty} h_k(\vec{z}_\perp, A) e^{ik\psi} : \right\} \\
&= \exp \left\{ - : \sum_{k=-\infty}^{\infty} h_k(\vec{z}_\perp, A) e^{ik(\psi - n\mu(A))} : \right\}
\end{aligned} \tag{3.10}$$

where $\mu(A)$ is the amplitude-dependent synchrotron phase advance, and we have used the fact that $\mathcal{M}_s \circ (A, \psi) = (A, \psi + \mu(A))$. We now need to compute the product in eqn. (3.9) as a single exponential operator to first order using the BCH formula from Appendix A to compute the stroboscopic Hamiltonian and its first order correction.

To construct the single exponential operator, we will rely on the BCH formula and a recursion relation defined by concatenating the first M terms from the right of the product in eqn. (3.9) with the next map to its left. Specifically, let us write the product as

$$\prod_{n=N}^1 \tilde{\mathcal{M}}_\perp^{(n)} = \left(\prod_{n=N}^{M+1} \tilde{\mathcal{M}}_\perp^{(n)} \right) \hat{\mathcal{M}}_\perp^{(M)} \tag{3.11}$$

where

$$\hat{\mathcal{M}}_\perp^{(1)} = \tilde{\mathcal{M}}_\perp^{(1)} \tag{3.12}$$

and

$$\hat{\mathcal{M}}_\perp^{(M+1)} = \tilde{\mathcal{M}}_\perp^{(M)} \hat{\mathcal{M}}_\perp^{(M)} \tag{3.13}$$

so that we end with

$$\hat{\mathcal{M}}_\perp^{(N)} = \prod_{n=N}^1 \tilde{\mathcal{M}}_\perp^{(n)}. \tag{3.14}$$

The goal is therefore to write

$$\hat{\mathcal{M}}_\perp^{(M)} = \exp \left\{ - : \hat{H}^{(M)} : \right\} \tag{3.15}$$

and compute $\hat{h}^{(M)}$ perturbatively using the BCH series.

From the BCH series, we can derive a recursion relation for \hat{h} to leading order in the Poisson brackets as

$$\hat{H}^{(M+1)} = \hat{H}^{(M)} + \sum_{k=-\infty}^{\infty} h_k(\vec{z}_\perp, A) e^{ik(\psi - M\mu(A))} + \varepsilon \frac{1}{2} \left[\hat{H}^{(M)}, \sum_{k=-\infty}^{\infty} h_k(\vec{z}_\perp, A) e^{ik(\psi - n\mu(A))} \right] + \mathcal{O}(\varepsilon^2) \tag{3.16}$$

where we have included ε to bookkeep the order in Poisson brackets.

Thus to order $\varepsilon = 0$, the stroboscopic Hamiltonian for the N -turn map is

$$\begin{aligned}
\hat{H}^{(N)} &= \sum_{m=1}^N \sum_{k=-\infty}^{\infty} h_k(\vec{z}_{\perp}, A) e^{ik(\psi - m\mu(A))} \\
&= \sum_{k=-\infty}^{\infty} \sum_{m=1}^N h_k(\vec{z}_{\perp}, A) e^{ik(\psi - m\mu(A))} \\
&= \sum_{k=-\infty}^{\infty} h_k(\vec{z}_{\perp}, A) e^{ik\psi} \left(\sum_{m=1}^N e^{-ikm\mu(A)} \right) \\
&= \sum_{k=-\infty}^{\infty} h_k(\vec{z}_{\perp}, A) e^{ik\psi} e^{ik\mu(A)} \frac{1 - e^{ikN\mu(A)}}{1 - e^{ik\mu(A)}}
\end{aligned} \tag{3.17}$$

Thus, if $N\mu(A) = 2\pi K$ for some integer K – i.e. the synchrotron tune is given by $\nu_s = K/N$ for the amplitude A – then all but the $k = 0$ term vanishes in the sum and we are left with

$$\hat{H}^{(N)} = N \times \overline{H}(\vec{z}_{\perp}, A) \tag{3.18}$$

and the N -turn map is equivalent to N turns of synchrotron motion and N turns of the period-averaged Hamiltonian $\overline{H}(\vec{z}_{\perp}, A)$. Thus \overline{H} will be stroboscopically invariant.

If, however, $N\mu(A) = 2\pi + \eta$, we are left with a term for $k \neq 0$ of the form

$$\frac{1 - e^{ikN\mu(A)}}{1 - e^{ik\mu(A)}} = \frac{1 - e^{ik\eta}}{1 - e^{ik\mu(A)}} \propto \eta \tag{3.19}$$

for $\eta \ll 1$. Thus, the perturbation to the stroboscopic Hamiltonian is proportional to the irrational part of the synchrotron tune, which can be made arbitrarily small.

We have thus shown that $\overline{H}(\vec{z}_{\perp}, A)$ is a stroboscopic invariant with synchrotron motion so long as the synchrotron tune is rational, and the correction is proportional to the arbitrarily small irrational part of the synchrotron tune. Therefore, if $\overline{H}(\vec{z}_{\perp}, A)$ is integrable, then the stroboscopic dynamics will be integrable to leading order.

Furthermore, the leading order term $N \times \overline{H}$ is $\mathcal{O}(\nu_s^{-1})$, since we defined N such that $N \times \nu_s \approx K$ and, since $\nu_s \ll 1$ we can assume that $K \ll N$. In Appendix B we show that the next leading order term is $\mathcal{O}(\nu_s^0)$ and oscillatory, and therefore the secular synchro-betatron dynamics is dominated by this stroboscopic Hamiltonian. To see this, we can cast the N -turn map as the N^{th} power of a single turn map:

$$\hat{\mathcal{M}}_{\perp}^{(N)} \sim \left(\hat{\mathcal{M}}_{\perp} \right)^N \tag{3.20}$$

with

$$\hat{\mathcal{M}}_{\perp} = \exp \left(- : \overline{H} + \varepsilon \frac{1}{N} h : \right) \tag{3.21}$$

where h is a bounded periodic function of the phase space variables. Thus, in the limit of large N , this term becomes perturbatively small compared to \overline{H} . This argument, that the oscillatory term does not lead to secular growth in the action, is analogous to the arguments described for averaging time-continuous Hamiltonian systems described in §19 of Arnold [16].

4 Stroboscopic Invariants in an Integrable Rapid-Cycling Synchrotron

To observe the existence of stroboscopic invariants in a complex system, we consider an integrable rapid-cycling synchrotron [17] (iRCS). This lattice design includes nonlinear integrable dynamics [4, 5], which intrinsically includes a tune spread with transverse amplitude designed to Landau damp coherent instabilities. Because our prior analysis is independent of the nature of the transverse Hamiltonian dynamics in the lattice, we expect to see two stroboscopic invariants of the motion.

To test this periodicity prediction, we computed the on-momentum ($A = 0$) Danilov-Nagaitsev invariants from [4] through many synchrotron oscillations. For small-amplitude synchrotron oscillations, we expect the effects of finite A to be perturbative, and we will see a synchrotron motion periodicity with the Danilov-Nagaitsev invariants.

Table 1 shows the key parameters for this lattice design. The phase advance through the nonlinear insert of $Q_0 = 0.3$, the nonlinear strength parameter is $t = 0.3$, and elliptic potential parameter is $c = 0.14 \text{ m}^{1/2}$. (see [4, 5]).

The iRCS is designed with 1.680 MV total RF voltage to provide to achieve a 20 Hz ramp rate and a 8 GeV extraction energy. In application, every other cell of the iRCS would contain RF cavities and the harmonic number for the ring would be 113. For modeling purposes, each of the twelve periodic cells has RF cavities providing 140 kV and the harmonic number for the ring is $9 \times 12 = 108$. To avoid transition crossing, the momentum compaction factor of the iRCS is designed to be 5.9×10^{-4} . At the injection energy 0.8 GeV, the synchrotron tune for the ring is 0.08 (and 0.007 per periodic cell).

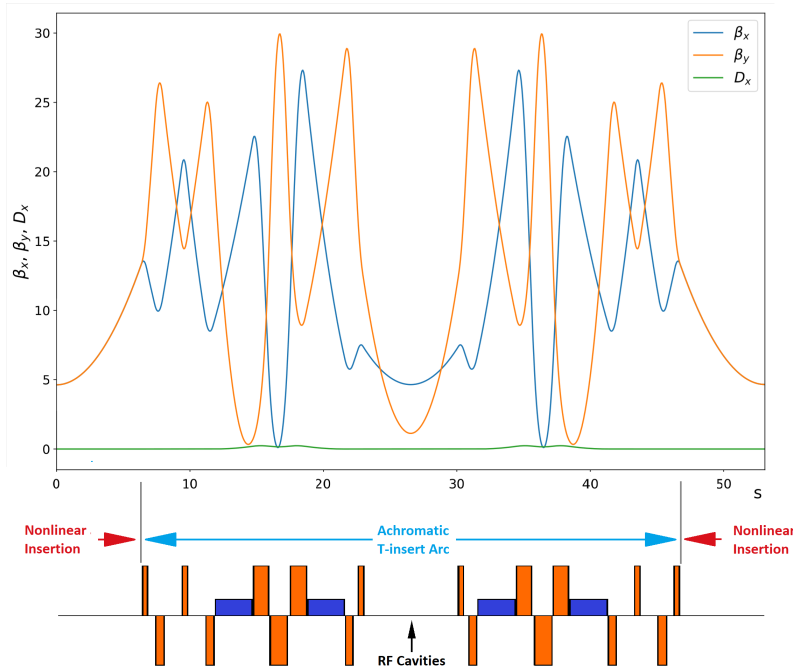


Figure 1. (top) Twiss parameters for one of the twelve periodic cells. (bottom) Beamline layout where dipoles are shown as short blue rectangles and quadrupoles as tall orange rectangles.

Table 1. Parameters of iRCSv3 Lattice

Parameter	Value
Circumference	636 m
Periodicity	12
Bend Radius	15.4 m
Max Beta Function	30 m
Max Dispersion	0.22 m
Betatron Tune	21.6
Linear Chromaticity	-79
Momentum Compaction	5.9×10^{-4}
Insertion lengths per cell	7.2 m, 4×1.3 m
RF Voltage	1.680 MV
Synchrotron Tune	0.08
NL Insertion Length	12.7 m
Phase-advance over insert	$0.3 \times \pi$
Nonlinear Strength t-value	0.3
Elliptic Distance c-value	$0.14 \text{ m}^{\frac{1}{2}}$
95% Transverse Emittance	20 mm mrad
95% Longitudinal Emittance	0.09 eV·s
Vertical Lattice Tune Spread	0.52
Horizontal Lattice Tune Spread	0.34
Chromatic Tune spread	0.52

The iRCS lattice was optimized to control the discrepancy between the horizontal and vertical tune across the momentum span $\pm 0.5\%$ without the use of sextupoles. The iRCS lattice also has the flexibility to finely adjust the betatron tune-matching and chromaticity matching independently. Figure 2 shows the tune dependence on momentum, measured by tracking the small-amplitude betatron oscillation of off-momentum particles, with the strength of the elliptic element set to zero.

The chromaticity combined with the nonlinear integrable optics makes the iRCS lattice a fairly complex example of synchro-betatron coupling.

In fig. (3) we plot the particle momentum offset and on-momentum Danilov-Nagaitsev invariants against the turn number T times the zero-amplitude synchrotron tune ν_s . As we can see, there is oscillatory behavior in the invariants periodic with the synchrotron oscillation, indicating the existence of a stroboscopic invariant. We can also see that this is in a regime where there is a finite amplitude-dependent synchrotron tune depression, as the successive minima in the top plot of fig. (3) are slightly greater than $T \times \nu_s = 1$ separated, indicating that $\nu_s(A) > \nu_s(0)$.

This periodicity is consistent over many hundreds of synchrotron periods, and across many initial particle trajectories. That persistence without secular growth indicates the presence of stroboscopic invariants in the Danilov-Nagaitsev Hamiltonian with synchrotron motion and chromatic effects.

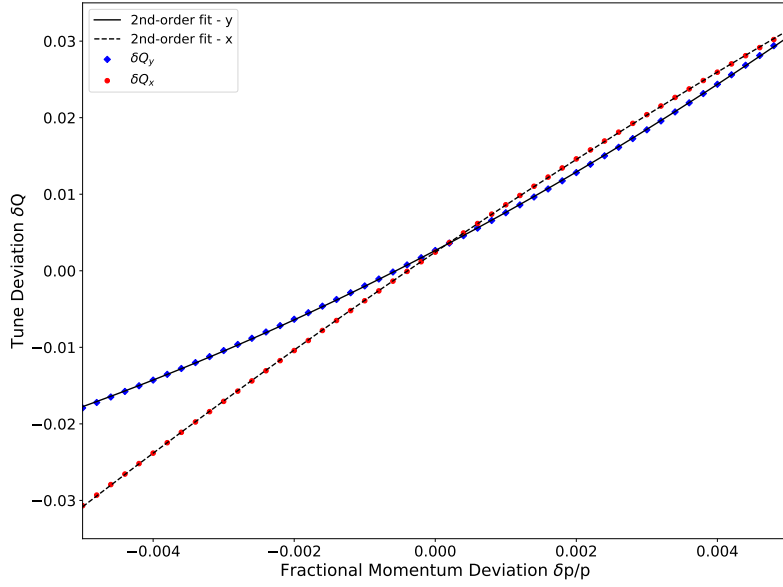


Figure 2. Vertical and horizontal chromaticities are plotted for a single cell of the 12-cell iRCS design.

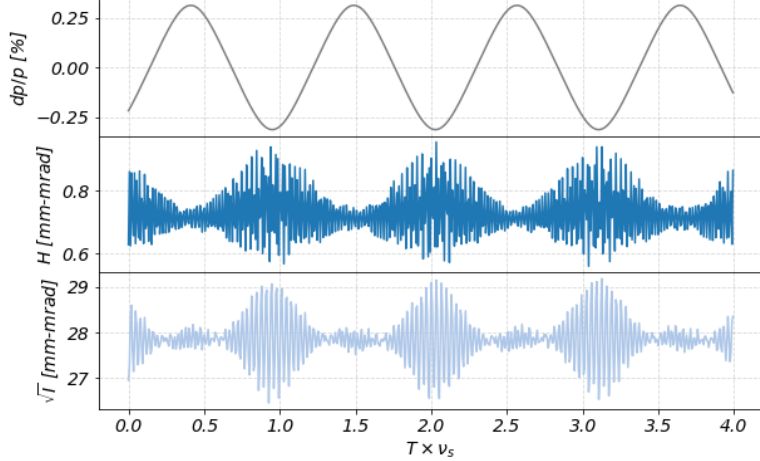


Figure 3. Sample trajectory showing oscillations in the on-momentum invariants in an integrable RCS.

5 Discussion

We have presented an approach to computing the N -turn map for an entire synchrotron period, and derived a stroboscopic Hamiltonian \overline{H} which defines the secular Hamiltonian dynamics of the full synchro-betatron coupling. The stroboscopic Hamiltonian is the average of the transverse Hamiltonian over a synchrotron period. This Hamiltonian is $O(\nu_s^{-1})$, with $\nu_s \ll 1$ the synchrotron tune, while the correction terms remain $O(1)$. Therefore, this holds well for small synchrotron tune. Furthermore, for multi-synchrotron-period maps, these correction terms will oscillate with

the number of periods, while the stroboscopic Hamiltonian term will grow linearly, suggesting that it dominates the long-term dynamics. We presented evidence of this stroboscopic Hamiltonian in the context of an integrable optics rapid cycling synchrotron, showing that the on-momentum Danilov-Nagaitsev invariants vary with momentum offset, but are periodic with the synchrotron period. The result, however, is generic to any Hamiltonian for the transverse dynamics, so long as a single Hamiltonian which generates the single-turn map for the transverse dynamics exists, i.e. in the absence of chaos.

A Symplectic Maps, Lie Algebras, and the Baker-Campbell-Hausdorff Formula

In this Appendix we will overview the mathematics of symplectic maps and Lie operators, highlighting key mathematical identities that we will use in this paper. Much of this is a survey of prior work by Dragt and others [8–14] as it pertains to the work presented here. We omit proofs for the sake of brevity, opting to state the relevant identities.

Given a Hamiltonian H , the equations of motion for a particle's phase space trajectory will satisfy the Poisson bracket differential equation

$$\frac{d\vec{z}}{dt} = -[H, \vec{z}] \quad (\text{A.1})$$

We can interpret $[H, \star]$ as a *Lie operator* that acts on $\vec{z}, :H:$. This implies that the evolution of \vec{z} can be cast as an operator differential equation, with the flow $\vec{z}_f = \mathcal{M}_{i \rightarrow f} \vec{z}_i$. This leads to the operator differential equation for the symplectic map \mathcal{M} which describes the flow for the Hamiltonian H :

$$\frac{d}{dt} \mathcal{M}_{t_i \rightarrow t} = - :H: \mathcal{M}_{t_i \rightarrow t} \quad (\text{A.2})$$

with the initial condition $\mathcal{M}_{t_i \rightarrow t_i} = \mathcal{I}$, the identity. \mathcal{M} contains all of the dynamics for the Hamiltonian H . We can solve this operator equation by iterative integration, i.e.

$$\mathcal{M}_{t_i \rightarrow t} = \mathcal{I} - \int_{t_i}^t dt' :H: \mathcal{M}_{t_i \rightarrow t'} \quad (\text{A.3})$$

Assuming H is independent of time, the solution can be written as the exponential operator

$$\begin{aligned} \mathcal{M}_{t_i \rightarrow t} &= \sum_{n=0}^{\infty} \frac{(-1)^n}{n!} (t - t_i)^n :H:^n \\ &\equiv \exp \{ - :H: (t - t_i) \} \end{aligned} \quad (\text{A.4})$$

where $:H:^n$ is defined as repeated application of the operator $:H:$. Operator exponentials play an important role in Lie algebraic treatments of symplectic maps.

In a particle accelerator, a symplectic map describes the change of phase space coordinates at the exit of the element given the coordinates at the entrance of the element:

$$\vec{z}_{\text{out}} = \mathcal{M}_i \circ \vec{z}_{\text{in}} \quad (\text{A.5})$$

In a ring, the product of all of these symplectic maps forms the *single-turn map*

$$\mathcal{M} = \prod_i \mathcal{M}_i \quad (\text{A.6})$$

which contains the full dynamics of the ring. Computing this single-turn map is the subject of normal form analysis and Taylor and Cremona polynomials, as well as, indirectly, the goal of tracking codes. For the purposes of this paper, we assume that we have already calculated the single-turn map, and that it is of the form

$$\mathcal{M} = e^{-:H:} \quad (\text{A.7})$$

where $-H$ is the generator of the map. This Hamiltonian is related to the invariants of motion, such as the Courant-Snyder invariants or the Danilov-Nagaitsev Hamiltonian.

The computation in this paper relies on two identities for these maps: the similarity transformation, and the Baker-Campbell-Hausdorff formula.

The similarity transform states that

$$\mathcal{G}^{-1} : f : \mathcal{G} = : \mathcal{G} f : . \quad (\text{A.8})$$

This identity frequently appears in the context of coordinate transformations, but in our case arises as we move all the synchrotron motion maps to the left. It is straightforward to show that

$$\mathcal{G}^{-1} : f :^n \mathcal{G} = : \mathcal{G} f :^n . \quad (\text{A.9})$$

by judicious insertion of $\mathcal{G}\mathcal{G}^{-1}$ between each instance of $: f :$, and we can therefore see that

$$\mathcal{G}^{-1} e^{:f:} \mathcal{G} = e^{:\mathcal{G}f:} \quad (\text{A.10})$$

The Baker-Campbell-Hausdorff (BCH) formula tells how to combine two non-commuting exponential Lie maps into one exponential Lie map, by providing a series for the generator of that combined Lie map. If we want to write the product of two exponential Lie maps as a single exponential Lie map, $e^{:f:} e^{:g:} = e^{:h:}$, then the BCH formula tells us the series for h in terms of f and g :

$$h = f + g + \frac{1}{2}[f, g] + \frac{1}{12}([f, [f, g]] - [g, [f, g]]) + \dots \quad (\text{A.11})$$

Although this is a formal power series, it may be asymptotic and indeed may not converge at all. We therefore need $[f, g]$ to be in some sense ‘‘small’’. This can mean multiple things, and the BCH series can be a perturbation series in, for example, powers of \vec{z} in the multipole picture of particle accelerators, or in this case the synchrotron tune, as we discuss in Appendix B.

B Leading Order Correction

To compute the next-leading order term for finite synchrotron tune, we need to go to the next order in the BCH series. We will truncate the series at $O(\varepsilon)$, so that we only consider single pairwise Poisson brackets. From eqn. (3.16), we can add a term so that we are computing $\hat{H}^{(M)} + \varepsilon P^{(M)}$, where P is the next order Poisson bracket term. This immediately gives the recursion relation

$$P^{(M+1)} = P^{(M)} + \frac{1}{2} \left[\hat{H}^{(M)}, \sum_k h_k e^{ik(\psi + M\mu)} \right] \quad (\text{B.1})$$

with the initial condition that $P^{(1)} = 0$. Therefore, we have that

$$P^{(N)} = \frac{1}{2} \sum_{n=1}^N \left[\hat{H}^{(n)}, \sum_k h_k e^{ik(\psi+n\mu)} \right] \quad (\text{B.2})$$

and furthermore, from our solution of the leading order Hamiltonian $\hat{H}^{(n)}$, we have

$$P^{(N)} = \frac{1}{2} \sum_{n=1}^N \sum_{m=1}^n \sum_{k,k'} \left[h_{k'} e^{ik'\psi} e^{ik'm\mu}, h_k e^{ik\psi} e^{ikn\mu} \right]. \quad (\text{B.3})$$

For clarity, define $f_k = h_k e^{ik\psi}$ and get that

$$P^{(N)} = \frac{1}{2} \sum_{n=1}^N \sum_{m=1}^n \sum_{k,k'} \left[f_{k'} e^{ik'm\mu}, f_k e^{ikn\mu} \right] \quad (\text{B.4})$$

The $(k, k') = 0$ term vanishes, so the only surviving terms in this correction oscillate in harmonics of the synchrotron period, due to the $e^{iq\mu}$ -type terms in the series. This means that this perturbation remains $\mathcal{O}(v_s^0)$, compared to the $\mathcal{O}(v_s^{-1})$ of the stroboscopic Hamiltonian.

Acknowledgments

This work was supported by the United States Department of Energy, Office of Science, Office of High Energy Physics under contract no. DE-SC0011340 and by [JEFF SUPPORT HERE].

References

- [1] C. L. Hammer, R. W. Pidd, and K. M. Terwilliger. Betatron Oscillations in the Synchrotron. *Rev. Sci. Instr.*, 26(555), 1955. doi: 10.1063/1.1715241.
- [2] Yu. F. Orlov. Excitation of Betatron Oscillations by Synchrotron Momentum Oscillations in a Strong Focusing Accelerator. *Soviet Phys. JETP*, Vol: 5, 1957.
- [3] S. Y. Lee. Single particle dynamics at synchro-betatron coupling resonances. *Phys. Rev. E*, 49(5706), 1994. doi: 10.1103/PhysRevE.49.5706.
- [4] V. Danilov and S. Nagaitsev. Nonlinear accelerator lattices with one and two analytic invariants. *Phys. Rev. ST Acc. Beams*, 13(084002), 2010.
- [5] S. Nagaitsev, A. Valishev, and V. Danilov. Nonlinear optics as a path to high-intensity circular machines. In *Proceedings of HB2010*, number THO1D01, 2010.
- [6] S. Nagaitsev and V. Danilov. A search for integrable four-dimensional nonlinear accelerator lattices. In *Proceedings of IPAC '10*, number THPE094, 2010.
- [7] S. Nagaitsev and A. Valishev. Description of nonlinear elements for the integrable optics test accelerator. FNAL Note, Nov. 2010.
- [8] A. Dragt and D. T. Abell. Symplectic Maps and Computation of Orbits in Particle Accelerators. In J. E. Marsden, G. W. Patrick, and W. F. Shadwick, editors, *Integration Algorithms and Classical Mechanics*, volume 10. American Mathematical Society, 1996.

- [9] A. Dragt and J. Finn. Lie series and invariant functions for analytic symplectic maps. *J. Math. Phys.*, 17(12), 1976.
- [10] A. Dragt and E. Forest. Computation of nonlinear behavior of Hamiltonian systems using Lie algebraic methods. *J. Math. Phys.*, 24(12), 1983.
- [11] A. Dragt. *Lie Methods for Nonlinear Dynamics with Applications to Accelerator Physics*. University of Maryland, 2016.
- [12] A. Dragt. A Method of Transfer Maps for Linear and Nonlinear Beam Elements. *IEEE Trans. Nucl. Sci.*, NS-26(3), 1979.
- [13] Alex J. Dragt. Lectures on nonlinear orbit dynamics. In *Physics of High Energy Particle Accelerators*, volume 87, pages 147–313. AIP Publishing, 1982.
- [14] A. J. Dragt. Nonlinear lattice functions. In R. Donaldson and J. Morfín, editors, *Proceedings of the 1984 Summer Study on the Design and Utilization of the Superconducting Super Collider*, pages 369–372, 1984.
- [15] É. Forest. Dispersive lattice functions in a six-dimensional pseudo-harmonic-oscillator. *Phys. Rev. E*, 58(2):2481–2488, 1998.
- [16] V. I. Arnold. *Geometrical Methods in the Theory of Ordinary Differential Equations*. Springer, 1988.
- [17] J. Eldred and A. Valishev. Integrable RCS as a proposed replacement for the Fermilab Booster. In *AIP Conf. Proc.*, volume 1812, 2017. doi: 10.1063/1.4975901.